Cell Reports, Volume *37*

Supplemental information

Regulatory T cell differentiation is controlled by αKG-induced alterations in mitochondrial metabolism and lipid homeostasis

Maria I. Matias, Carmen S. Yong, Amir Foroushani, Chloe Goldsmith, Cédric Mongellaz, Erdinc Sezgin, Kandice R. Levental, Ali Talebi, Julie Perrault, Anais Rivière, Jonas Dehairs, Océane Delos, Justine Bertand-Michel, Jean-Charles Portais, Madeline Wong, Julien C. Marie, Ameeta Kelekar, Sandrina Kinet, Valérie S. Zimmermann, Ilya Levental, Laurent Yvan-Charvet, Johannes V. Swinnen, Stefan A. Muljo, Hector Hernandez-Vargas, Saverio Tardito, Naomi Taylor, and Valérie Dardalhon

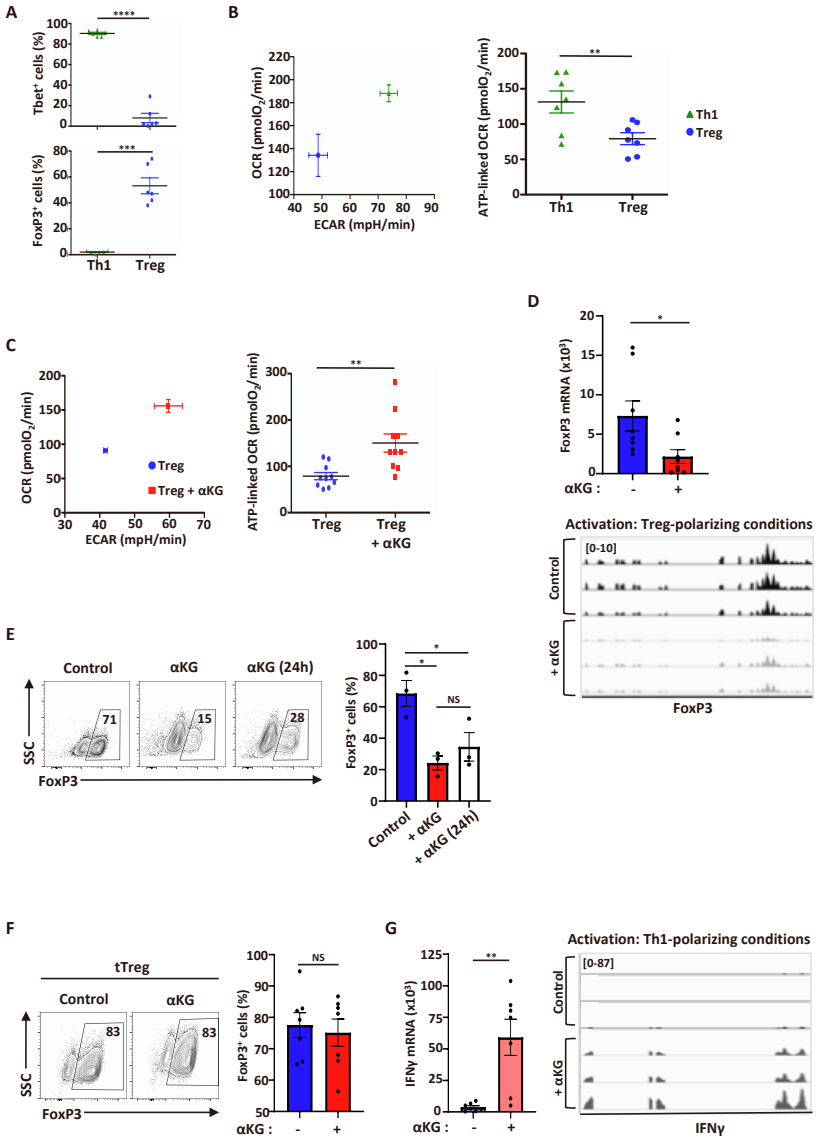

Figure S1. Treg polarization is attenuated by αKG. Related to Figure 1.
(**A**) The polarization of naïve CD4 T cells stimulated under Th1- and Treg-polarizing conditions was evaluated as a function of Tbet and FoxP3 expression, respectively. The percentages of Tbet$^+$ and FoxP3$^+$ cells were monitored by intracellular staining and individual data points from 6 independent experiments are presented. Means ± SEM are presented by horizontal lines (left panels). **(B)** Energy plots (left) of basal OCR and extracellular acidification rate (ECAR) as well as ATP-linked respiration (right, n=7 independent experiments, means ± SEM) are presented. **(C)** Naïve CD4 T cells were stimulated under Treg-polarizing conditions in the absence (control) or presence of αKG and OCR/ECAR energy plots (left) as well as ATP-linked OCR (right) are presented (n=10 independent experiments, means ± SEM). **(D)** *Foxp3* mRNA levels ± SEM were evaluated by qRT-PCR and normalized to *HPRT* (left, n=8). RNAseq read densities of the *Foxp3* gene were evaluated (n=2 independent experiments with technical triplicates). (**E**) αKG was added to naïve CD4 T cells stimulated under Treg-polarizing conditions at time 0 or at 24h. The percentages of FoxP3$^+$ cells were evaluated at day 4 and representative dot plots (left) as well as a quantification of the means ± SEM of 3 independent experiments are shown (right). **F**) FoxP3$^+$GFP$^+$ thymic Tregs (tTregs) were activated in the indicated conditions. At day 4, the percentages of FoxP3$^+$ cells were evaluated (left) and quantification of means ± SEM are presented (right, n=7). (**G**) Naïve CD4 T cells were stimulated under Th1-polarizing conditions and *Ifng* mRNA levels were assessed by qRT-PCR at day 4 of Th1 polarization (left panel, n=7). Genome browser shots of RNA-seq reads over the *Ifng* gene are shown with the range of reads per million (RPM) presented on the y axis (n=2 independent experiments with technical triplicates, right panel). Statistical differences were determined by a paired (panels A, B, C) or unpaired (panels D, F, G) 2-tailed t test (panels A, B, C), or a one-way ANOVA and Tukey multiple comparison test (panel E). *, p<0.05; **, p<0.01; ***, p<0.001; ****, p<0.0001; NS, not significant

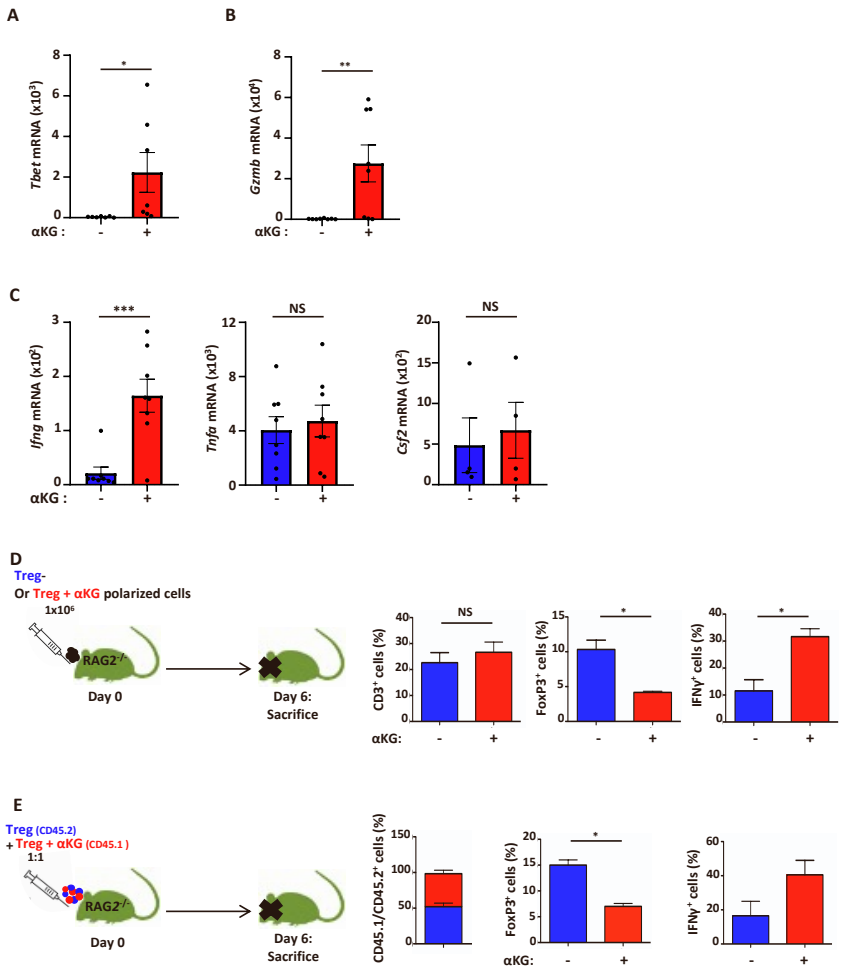

Figure S2. The altered potential of CD4 T cells polarized in the presence of αKG persists following adoptive transfer. Related to Figure 2.

(A) Following polarization of CD4 T cells under Treg conditions in the presence or absence of αKG (day 4), *T-bet* transcripts were quantified by qRT-PCR and normalized to *Hprt*. (n=7). **(B)** Granzyme B (*GzmB*) transcripts were quantified by qRT-PCR and normalized to *Hprt* (n=7). **(C)** mRNA levels for *Ifng* (n=8), *Tnfa* (n=8) and *Csf2* (GM-CSF, n=4*)* were assessed by qRT-PCR and normalized to *Hprt*. **(D)** RAG2$^{-/-}$ mice were adoptively transferred with CD4 T cells polarized in Treg conditions in the absence or presence of αKG (1e6) and mice were sacrificed at day 6 (schematic on the left). The percentages of CD3 T cells, FoxP3^{+} T cells and IFNγ^{+} T cells were evaluated by flow cytometry and means ± SEM are presented (n=3, right panels). (**E**) Mice were subjected to a competitive transfer of 0.5e6 CD4 T cell polarized in the absence (CD45.2) or presence of αKG (CD45.1) and evaluated at day 6 (schematic on the left). The percentages of CD45.1 and CD45.2 T cells as well as the percentages of FoxP3^{+} and IFNγ^{+} T cells are presented (n=3 and n=2 for FoxP3 and IFNγ respectively, means ± SEM, right panels). Each point in panels A-C represents an independent experiment with means ± SEM presented. Statistical differences were determined by an unpaired (panels A-C) or paired (panels D, E) 2-tailed t test. *, p<0.05; **, p<0.01; ***, p<0.001; NS, not significant

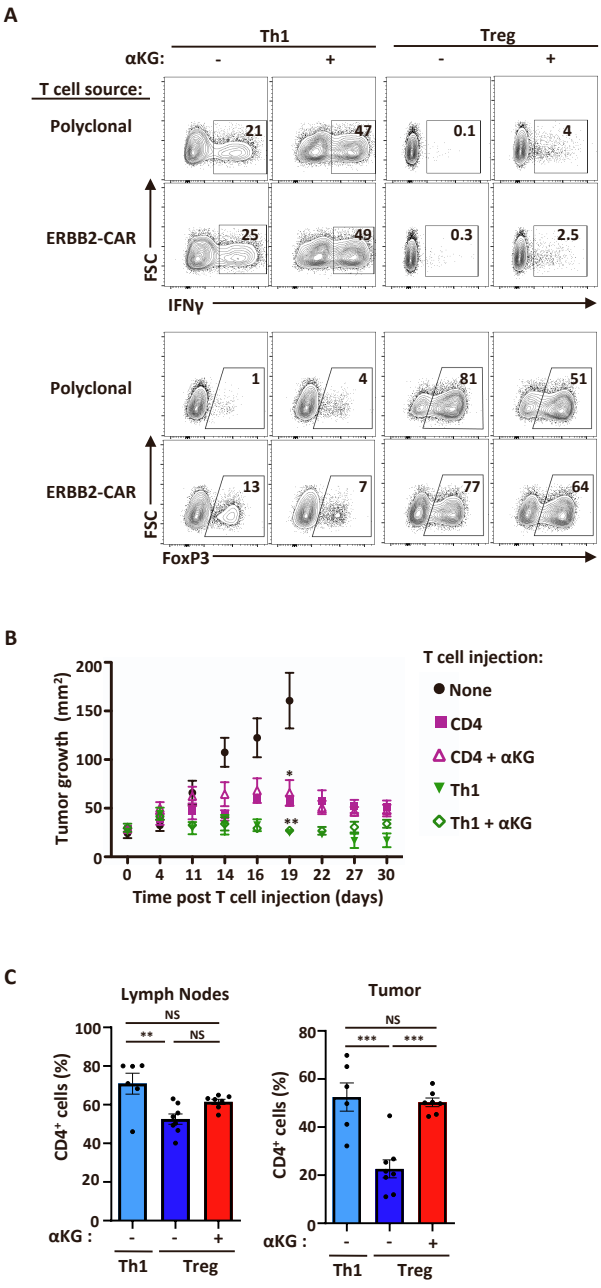

Figure S3. ERBB2-CAR T cells attenuate the growth of ERBB2$^+$24JK fibrosarcoma. Related to Figure 3.

(A) The potential of transgenic ERBB2-CAR T cells, as compared to polyclonal T cells, to be polarized to a Th1 or Treg fate was compared in the absence or presence of αKG. IFNγ production was evaluated at day 4 of stimulation in the indicated conditions and representative plots are shown (top plots). The induction of FoxP3 expression was also evaluated at day 4 and the percentages of FoxP3$^+$ cells are indicated (bottom plots). **(B)** ERBB2-CAR CD4 T cells were activated for 5 days in neutral or Th1-polarizing conditions in the absence of presence of αKG. They were adoptively transferred into RAG2$^{-/-}$ mice (3e6) that had been subcutaneously injected with ERBB2$^+$24JK fibrosarcoma 7 days earlier. Tumor volume was measured at the indicated time points. Mean tumor area ± SEM is presented from days 0 to 30 (n=4 mice per group) and statistical differences were evaluated at day 19. **(C)** Quantification ± SEM of CD4 T cells in LN (left) and tumor (right) were monitored with each point representing data from an individual mouse (n=6-8 per group). Statistical differences were determined by a one-way ANOVA and Tukey test for multiple comparisons. *, p<0.05; **, p<0.01; ***, p<0.001; ****, p<0.0001; NS, not significant

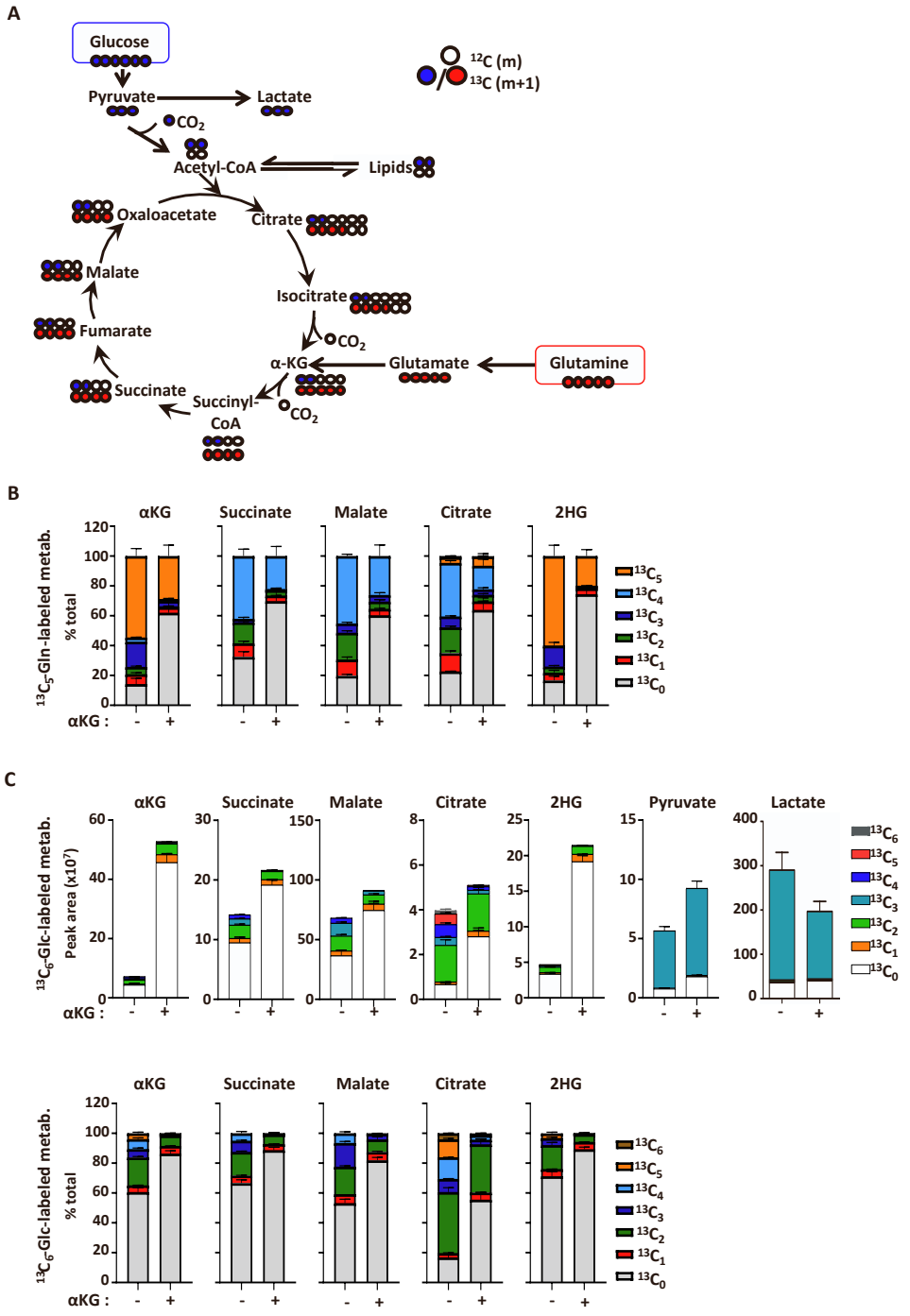

Figure S4. Utilization of glucose carbons for the generation of TCA cycle intermediates is decreased in the presence of αKG. Related to Figure 5.
(A) Schematic representation of ^{13}C labeling in TCA cycle intermediates generated from [$^{13}C_6$]glucose and [$^{13}C_5$]glutamine. **(B)** The mean fractional abundance of the different isotopologues from [$^{13}C_5$]glutamine into TCA cycle intermediates are shown as a percentage of the total. **(C)** The peak area of each metabolite and percentage incorporation of the carbon isotopologues from [$^{13}C_6$]glucose (top graphs) as well as the mean fractional abundance of the different isotopologues as a percentage of the total (bottom graphs) are shown. Quantifications are presented as means ± SEM (n=2 independent experiments, technical triplicates).

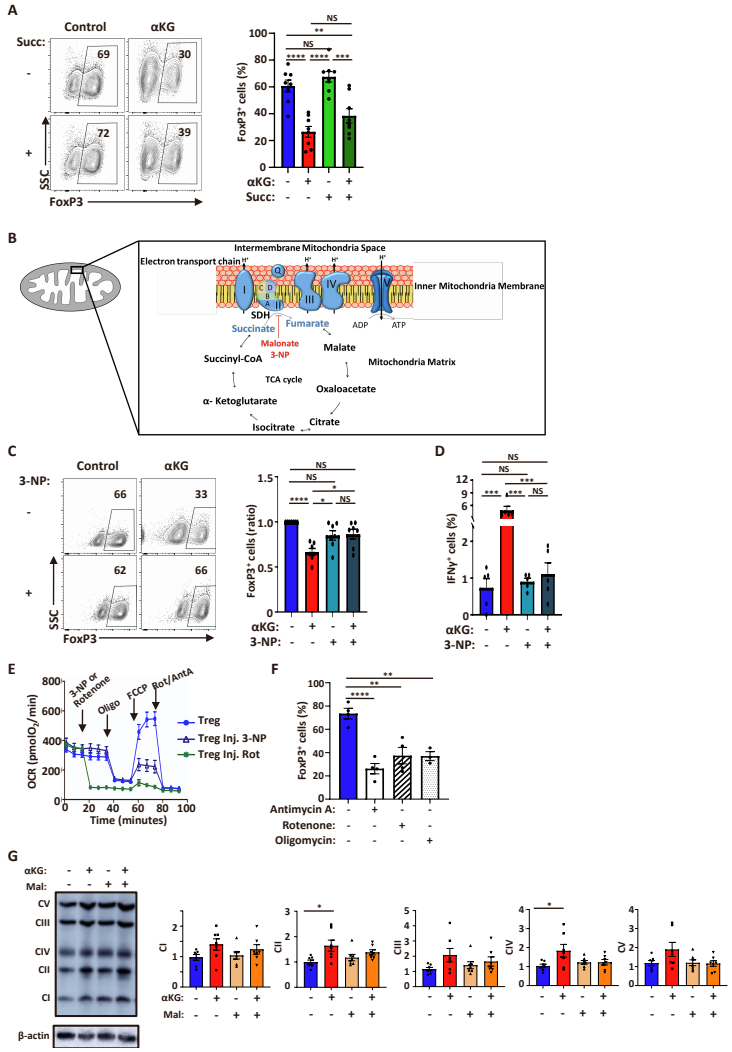

Figure S5. Inhibition of Complex II inhibits the αKG-mediated attenuation of Treg differentiation. Related to Figure 5.

(A) Naïve CD4 T cells were stimulated in Treg polarization conditions in the absence or presence of αKG and succinate as indicated (3.5 mM). The percentages of FoxP3$^+$ cells were evaluated at day 4 by intracellular staining and representative plots are shown (left). Quantification of FoxP3 levels is presented as means ± SEM of 7 independent experiments. **(B)** Schematic representation showing the role of the succinate dehydrogenase (SDH) enzyme in both the TCA cycle and the electron transport chain. Inhibitors (Malonate, 3-NP) of mitochondrial complex II (SDH) are indicated. **(C)** The impact of 3-NP (62.5μM) on Treg polarization was evaluated and representative FoxP3 plots (left) as well as the normalized ratio ± SEM of FoxP3$^+$ cells is presented (n=7, right). **(D)** The percentages of IFNγ^+ cells in the different conditions are presented (n=5, means ± SEM). **(E)** At day 4 of polarization under Treg conditions, oxygen consumption was monitored following injection (inj.) of 3-NP (62.5μM) or rotenone (100nM) directly into the Seahorse analyzer. OCR is also presented following injection of oligomycin, FCCP, and rotenone/antimycin A as indicated. Data are means of 4-6 replicates and are representative of 1 of 2 independent experiments. **(F)** The mean percentages ± SEM of FoxP3$^+$ cells differentiating in the presence of antimycin A (250nM), rotenone (25nM), and oligomycin (250nM, added at day 1) relative to control conditions are presented (n=3-4 independent experiments, day 4 of polarization). **(G)** Levels of mitochondrial complexes I-V were monitored using an antibody cocktail and representative levels together with an actin loading control are presented (left). Quantification of levels in 7 independent experiments was determined relative to actin and means ±SEM are presented. Significance was determined either by unpaired 2-tailed test (panels A and B) or by a one-way ANOVA and Tukey multiple comparison test (panels C-G). *, p<0.05; **, p<0.01; ***, p<0.001; ****, p<0.0001; NS, not significant)

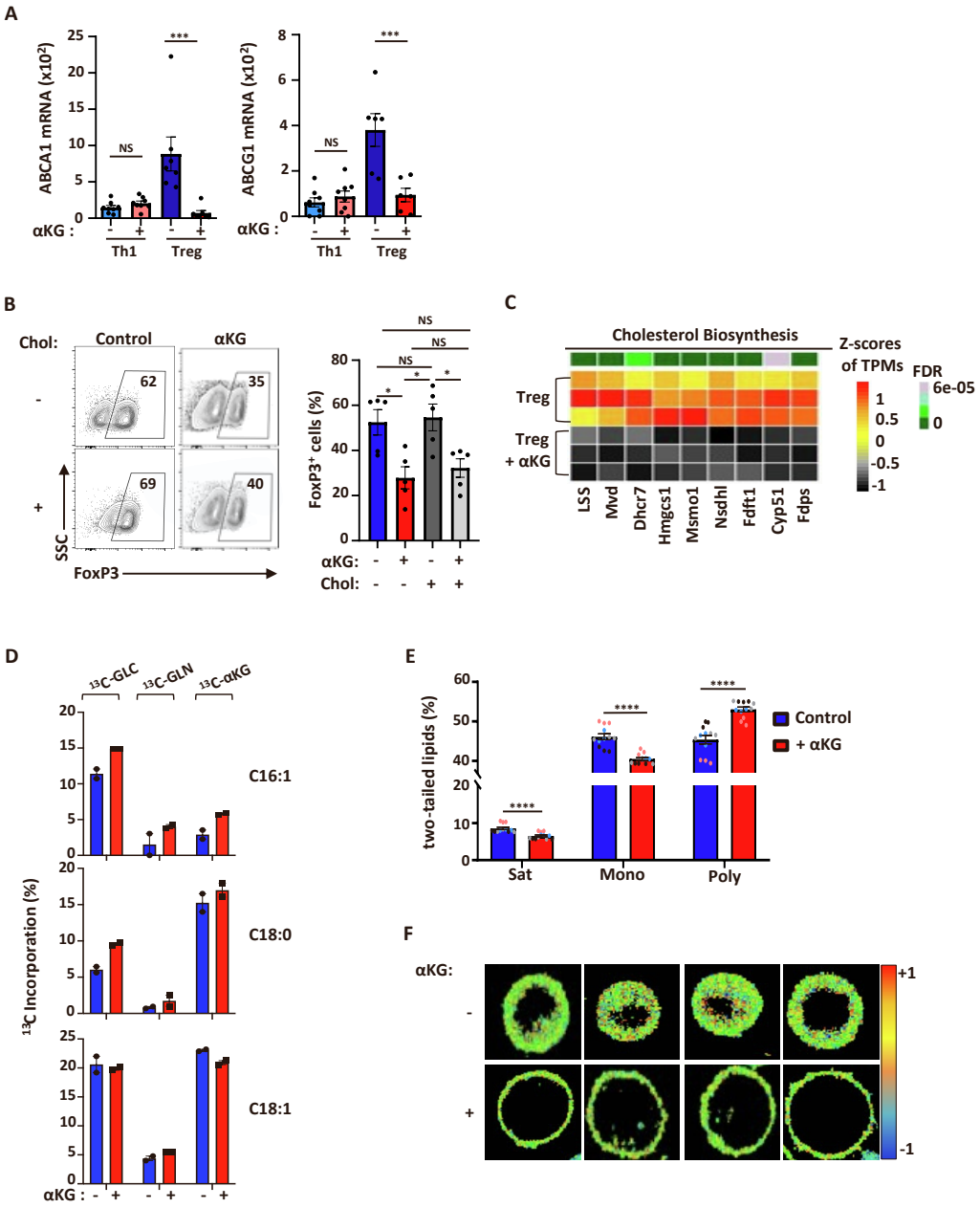

Figure S6. Decreased αKG-induced transcription of cholesterol-biosynthesis genes does not regulate Treg polarization. Related to Figure 6.
(A) *Abca1* and *Abcg1* transcripts were assessed by qRT-PCR and normalized to *HPRT*. Data are presented as means ± SEM of technical triplicates from 8 independent experiments. **(B)** Naïve CD4 T cells were activated in Treg polarizing conditions in the absence or presence of αKG and/or water-soluble cholesterol (50mM). The percentages of FoxP3$^+$ cells were evaluated on day 4 by intracellular staining and representative dot plots are presented (left) as well as a quantification of the means ±SEM of 5 independent experiments (right). **(C)** A heatmap of RNASeq data showing scaled expression (Z-scores of TPM transformed count data) for cholesterol biosynthesis genes in T cells activated in Treg-polarizing conditions in the absence or presence of αKG. Each row represents an independent sample. Statistical significance is indicated in the top bar. **(D)** The percent incorporation ± SEM of carbon isotopologues from [$^{13}C_6$]glucose, [$^{13}C_5$]glutamine, and [$^{13}C_5$]dimethyl-αKG into C16:1, C18:0, and C18:1 FAs is shown following Treg polarization in the presence or absence of αKG (n=2 technical replicates). **(E)** The level of unsaturation in membrane phospholipids (Sat, Saturated; Mono, Monounsaturated; Poly, Polyunsaturated) is presented as means ± SEM. **(F)** Representative C-Laurdan spectral microscopy evaluating packing of membranes as a function of the red shift in loosely packed membranes (means± SEM). Significance was determined by unpaired 2-tailed test *, p<0.05; ***, p<0.001; ****, p<0.0001; NS, not significant)

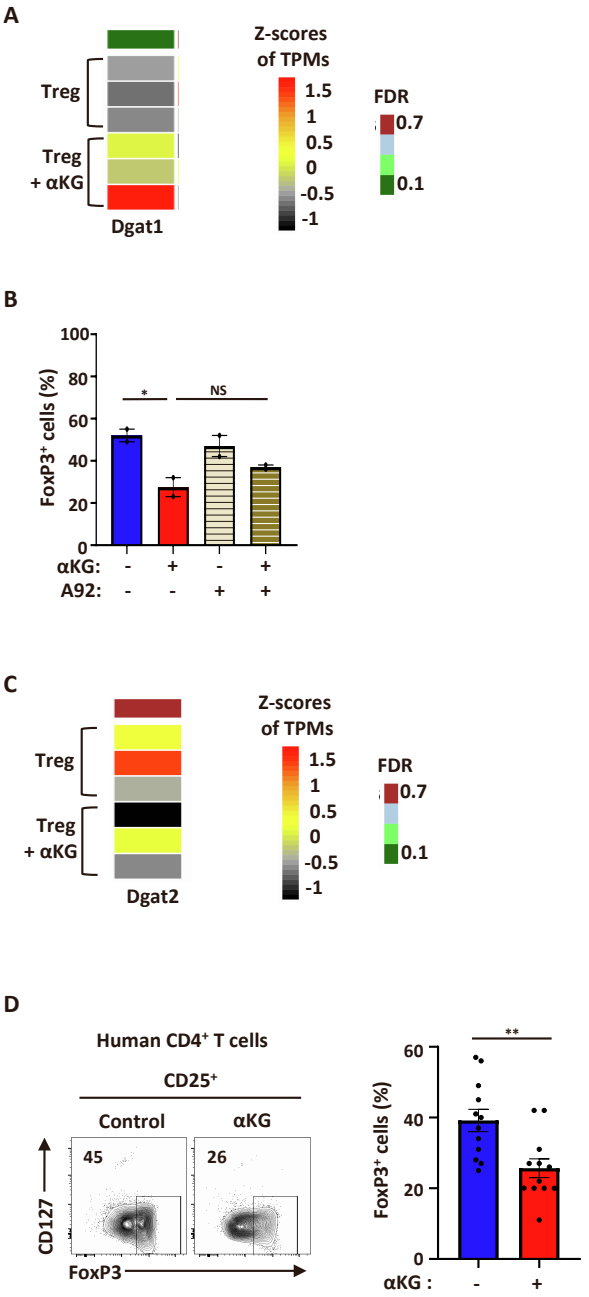

Figure S7. Inhibition of DGAT1 does not rescue Treg differentiation in the presence of αKG. Related to Figure 7.

(A) A heatmap of RNASeq data showing scaled expression (Z-scores of TPM transformed count data) for *Dgat1* in T cells activated in Treg-polarizing conditions in the absence or presence of αKG. Each row represents an independent sample and statistical significance is indicated in the top bar. **(B)** The impact of the DGAT1 inhibitor A-925200 (40μM) on Treg polarization was evaluated and the percentages of FoxP3$^+$ cells ± SEM are presented at day 4 (n=2). Statistical difference was determined by a one-way ANOVA and Tukey test for multiple comparisons (*, $p<0.05$; NS, not significant). **(C)** A heatmap of *Dgat2* RNASeq data is presented as for panel A. **(D)** Naïve human CD4$^+$ T cells were activated in Treg-polarizing conditions and at day 4 of stimulation, Treg polarization was evaluated as a function of intracellular FoxP3 staining in gated CD25$^+$CD127^{low} cells (left). Quantification ± SEM of the percentages of FoxP3$^+$ cells is shown for 12 healthy donors (12 independent experiments) and significance was determined by an unpaired t-test. **, $p=0.003$

Supplemental Table 5. Genes upregulated in enriched pathways following polarization in Treg conditions in the presence of αKG. Related to Figure 4.

Mitochondrial RNA metabolic process	Ribonucleoprotein complex biogenesis		Miitochondrial gene expression	ncRNA metabolic process		RNA modification
Aars2	Aatf	Nop58	Aars2	Aatf	Nsun5	Aars2
Elac2	Abce1	Npm1	Elac2	Abce1	Nufip1	Ctu2
Fastkd1	Bop1	Npm3	Fastkd2	Bop1	Pa2g4	Dimt1
Fastkd5	Brix1	Nsun5	Fastkd5	Brix1	Pdcd11	Dkc1
Lrpprc	Bysl	Nufip1	Gfm1	Bysl	Ppan	Elp1
Mrpl12	Dcaf13	Pa2g4	Lrpprc	Dcaf13	Prmt5	Ftsj3
Polrmt	Ddx21	Pdcd11	Mrpl12	Ddx21	Pwp2	Mettl1
Ppargc1b	Ddx27	Ppan	Mrpl47	Ddx27	Rcl1	Mettl16
Slc25a33	Ddx51	Prmt5	Mrps18b	Ddx51	Rpl7l1	Mrm1
Supv3l1	Ddx56	Pwp2	Mrps34	Ddx56	Rps27l	Nat10
Tbrg4	Denr	Rcl1	Polrmt	Denr	Rrn3	Nhp2
Trnt1	Dhx30	Rpl7l1	Ppargc1b	Dhx30	Rrp15	Nsun2
Twnk	Dhx37	Rps27l	Qrsl1	Dhx37	Rrp1b	Nsun5
Yars2	Dimt1	Rrn3	Slc25a33	Dimt1	Rrp7a	Pus1
	Dkc1	Rrp15	Supv3l1	Dkc1	Rrp8	Pus7
	Ebna1b	Rrp1b	Tbrg4	Ebna1bp2	Rrp9	Pus7l
	Eif3g	Rrp7a	Trnt1	Eif3g	Rrs1	Pusl1
	Eif6	Rrp8	Trub2	Eif6	Rsl24d1	Rpusd2
	Exosc1	Rrp9	Twnk	Exosc1	Sdad1	Thg1l
	Exosc0	Rrs1	Uqcc2	Exosc10	Srfbp1	Thumpd1
	Fastkd2	Rsl1d1	Yars2	Fastkd2	Surf6	Trmt1
	Fcf1	Rsl24d1		Fcf1	Tarbp2	Trmt6
	Ftsj3	Sdad1		Ftsj3	Tbl3	Trmt61a
	Gemin4	Srfbp1		Gemin4	Tsr1	Trub2
	Gemin5	Surf6		Gemin5	Urb1	
	Gnl2	Tarbp2		Gnl2	Urb2	
	Gtpbp4	Tbl3		Gtpbp4	Usp36	
	Heatr1	Tsr1		Heatr1	Utp14a	
	Heatr3	Urb1		Heatr3	Wdr12	
	Hsp90aa1	Urb2		Hsp90aa1	Wdr18	
	Imp4	Usp36		Imp4	Wdr43	
	Ipo4	Utp14a		Ipo4	Wdr46	
	Lyar	Wdr12		Lyar	Wdr74	
	Mdn1	Wdr18		Mphosph10	Wdr75	
	Mettl16	Wdr43		Mrm1	Zfp593	
	Mphosph10	Wdr46		Mrpl11	Znhit3	
	Mrm1	Wdr55		Mrto4	Znhit6	
	Mrpl11	Wdr74		Mybbp1a		
	Mrto4	Wdr75		Nat10		
	Mybbp1a	Zfp593		Ncl		
	Nat10	Znhit3		Nhp2		
	Ncl	Znhit6		Nip7		
	Nhp2			Nle1		
	Nip7			Nob1		
	Nle1			Noc4l		
	Nob1			Nol10		
	Noc4l			Nol6		
	Nol10			Nol9		
	Nol6			Nop14		
	Nol8			Nop16		
	Nol9			Nop56		
	Nop14			Nop58		
	Nop16			Npm1		
	Nop56			Npm3		

Supplemental Table 6. Genes downregulated in enriched pathways following polarization in Treg conditions in the presence of αKG. Related to Figure 6.

Cellular response to lipoprotein particle stimulus	Response to lipoprotein particle	Adaptive thermogenesis	Steroid metabolic process	Neg. regulation-intracellular signal transduction
Abca1	Abca1	Ache	Abca1	Arhgap12
Abcg1	Cd81	Arntl	Abcg1	Arntl
Cd81	Hmgcs1	Arrdc3	Adm	Arrdc3
Hmgcs1	Itgb1	Ddit3	Aplp2	Bcl6
Itgb1	Ldlr	Elovl6	Cat	Ccn3
Ldlr	Pparg	Epas1	Cyp51	Cgnl1
Pparg	Srebf2	Grb10	Dab2	Cpne1
Srebf2	Syk	Igf1r	Dhcr7	Dab2
Syk		Il18r1	Esr1	Dab2ip
		Ip6k1	Fdft1	Ddit3
		Lpin1	Fdps	Dhx58
		Map2k6	Hmgcr	Dmd
		Ogt	Hmgcs1	Dusp1
		Oxtr	Hsd17b7	Dusp6
		Plcl1	Igf1r	Epm2a
		Pparg	Igfbp7	Esr1
		Prlr	Insig1	G2e3
		Scd1	Ldlr	Hdac7
		Syk	Ldlrap1	Herpud1
		Vegfa	Lss	Hmgcr
		Zfp516	Msmo1	Igf1r
			Mvd	Inpp5k
			Mvk	Itgb1
			Nsdhl	Klf4
			Plekha1	Mcl1
			Pmvk	Myadm
			Rora	P2rx7
			Sc5d	Pde4b
			Scd1	Phlpp1
			Sqle	Pik3ip1
			Srebf1	Pink1
			Srebf2	Plekha1
			Stard4	Pttg1ip
			Tm7sf2	Rasa1
				Rasa3
				Rnf152
				Rora
				Rtkn2
				Sh3bp4
				Socs2
				Spry1
				Timp3
				Ube2b
				Ubr2
				Wtip

Supplementary Table 7. Cas9–crRNA Guides. Related to STAR Methods

Locus	Probe_ID		Sequence (mm10)	PAM	On-Target Score	Off-Target Score
Itgb8	itgb8_up_hh	-	CGATTACCTCTATCCTACAA	AGG	76	84
	itgb8_down_hh	+	AGTGGAAGTGTCCTGTACAA	TGG	94	54
Foxp3	FoxP3_down2.1	-	ACGGTGGAATTGCTGCCTGA	TGG	57	68
	FoxP3_down2.2	-	ATGGACTGCCCTGATAGATA	GGG	62	57
IL17a	il17a_down	-	TGTGGAACCTAAACACACGA	GGG	82	73
	il17a_up	+	CTAGCTTTACCAATTCCATA	AGG	75	46
Rorc	rorc_down	-	AAGACCTAACTACCTAGCAC	AGG	85	44
	rorc_up	+	GATAAGAGGACTGGGCACGT	GGG	76	71
Ifng	ifng_up	+	GCATCTGGGTCAAGATAACT	GGG	75	61
	ifng_down	-	CAATGCCTTTCCAAGGGTAT	TGG	71	50
Il10	il10_up	+	GACCTCACATAAGGTTCTTG	AGG	74	68
	il10_down	-	GCAAGCCTGACATTGACGTG	CGG	64	77
Maf	Maf_up	+	GGAAAGCTATCACACCTGTT	TGG	78	50
	Maf_down	-	CCATTTGAGCCTGACGTCAC	GGG	77	46
Il4	IL-4_up	+	GTTCTTGTTTCACAAGCCGC	AGG	52	72
	IL-4_down	-	GGGGCAATGAGTACCTCGAC	AGG	73	88
Gata3	GATA3_up	+	AAGCTTGTAGTACAGCCCAC	AGG	77	67
	GATA3_down	-	GTTAGTTGTACACGGTACTT	CGG	65	86

On/Off Target Scores are based on IDT's web design tool:

https://eu.idtdna.com/site/order/designtool/index/CRISPR_PREDESIGN

PAM = protospacer adjacent motif